

Title	FEM Simulation of Spot Welding Process (Report I) : Effect of Initial Gap on Nugget Formation(Mechanics, Strength & Structure Design)
Author(s)	Murakawa, Hidekazu; Zhang, Jianxun
Citation	Transactions of JWRI. 1998, 27(1), p. 75-82
Version Type	VoR
URL	<a href="https://doi.org/10.18910/7780">https://doi.org/10.18910/7780</a>
rights	
Note	

*Osaka University Knowledge Archive : OUKA*

<https://ir.library.osaka-u.ac.jp/>

Osaka University

# FEM Simulation of Spot Welding Process (Report I)<sup>†</sup>

—Effect of Initial Gap on Nugget Formation—

Hidekazu MURAKAWA\* and Jianxun ZHANG\*\*

## Abstract

*The initial gap between the press formed components of thin plate to be welded by spot welding process is an inevitable problem. A numerical simulation model for spot welding process with initial gap has been constructed and is based on the finite element method as a thermal elastic-plastic problem. The contact states and nugget formation of a mild steel were analyzed for spot welding with initial gap. The conclusions show that a ring-like contact state can be formed between electrode and plate under the static squeezing force, and then it will develop from two sides (outside and inside) as welding time increases. The initial formation of the nugget is delayed by the initial gap. The effects of welding current and squeezing force on the nugget formation were investigated.*

**KEY WORDS:** (Spot Welding) (Finite Element Method) (Initial Gap)

## 1. Introduction

The spot welding process is widely used to join the sheet metal components in the mass production industries like the automotive industry, the electronic industry and so on. It is important to keep a stable, good quality of welded joint for the extensive use of the spot welding process. The experimental and theoretical analyses dealing with temperature distributions, nugget formation and influential factors have been conducted by many researches<sup>1-4</sup>. Compared with experimental methods, the computer simulation based on various numerical methods is becoming more and more popular in investigations of the spot welding process because of its reduced cost, rising speed of computation and the capability for separating the effects of many factors involved in the process. The first heat conduction model was introduced to simulate the spot welding process by using the finite difference method<sup>5</sup>. This was considered a significant contribution to the numerical modeling efforts of spot welding process. A coupled axisymmetric model using the finite element code ANSYS<sup>6</sup> was proposed to predict the deformation of electrode and workpiece. In that analysis, the geometry of electrode

and workpiece, temperature dependent thermal properties and melting of workpiece were considered. Based on the same finite element code ANSYS, the weld nugget in resistance spot welding of Type 347 stainless steel with uniform and variable thicknesses was found to initiate in a ring shape at a distance from the electrode center and to expand inward and outward during welding cycles<sup>7</sup>. The relationship was studied numerically for various welding conditions and weldabilities of aluminum alloy in spot welding by self-developed finite element code<sup>8</sup>. A real-time control methodology, expansion-based control algorithm, in spot welding has been developed, in which the finite element method was used to simulate the welding process<sup>9</sup>. Direct correlations between nugget formation and expansion displacement between electrodes were obtained.

The initial gap between plates is an inevitable problem in spot welding of thin plates. The use of high tensile strength steel increases the tendency for an initial gap to be formed because the press formability of the high tensile strength steel is relatively poor compared to that of mild steel. It is reported that the weldability, with respect to the nugget formation, is strongly governed by the contact states of both electrode to plate

<sup>†</sup> Received on June 1, 1998

\* Associate Professor

\*\* Foreign Research Fellow,  
(Professor, Xi'an Jiaotong University)

Transactions of JWRI is published by Joining and Welding Research Institute of Osaka University, Ibaraki, Osaka 567-0047, Japan.

and plate to plate, and appropriate welding conditions to improve the weldability were proposed<sup>10</sup>).

The deformation under squeezing processes in spot welding with a gap were analysed using a finite element method. On the basis of the numerical analysis, the squeezing process can be divided into three stages with respect to plastic deformation and large deformation. Further, to predict the electrode force required to close the initial gap, two methods, using parametric curves and approximation curves respectively, have been proposed<sup>11</sup>).

In this report, a numerical simulation model for the spot welding process with an initial gap has been conducted using the finite element method based on a thermal elastic-plastic theory. The change of contact states of electrode to plate and that of plate to plate, also the effects of the initial gap on the formation of nugget have been analyzed, taking the welding current and squeezing force into account.

2. Numerical Procedure and Model

The spot welding involves the electric field problem, the heat conduction problem and the thermal elastic-plastic deformation problem. In addition to these, the change of contact states between electrode/plate and plate/plate must be considered. To solve this type of coupled problem in a strict manner, simultaneous solutions of the electric, the thermal and the mechanical fields are necessary. However, due to the complexity and the cost of the analysis, an alternative approximate method is employed in the present report. Instead of solving the three fields simultaneously, they are solved sequentially with respect to small time increment as follows.

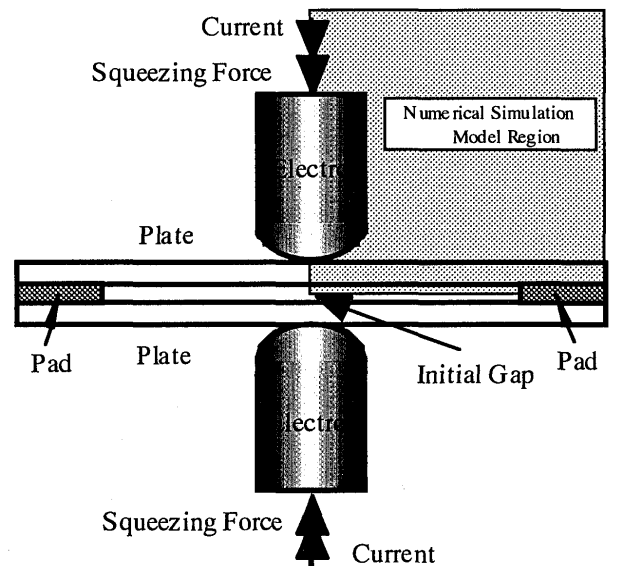
- (1) calculating the contact state.
- (2) calculating the electric field with temperature dependent material constants.
- (3) calculating the temperature field according to the electric field computed in stage (2), considering temperature dependent material constants.
- (4) calculating the deformation, the contact state and the nugget formation for the temperature increment.
- (5) return to stage (2) and continue the same cycle until the welding process is completed.

A spring-type interface element is introduced to simulate the contact states of the interfaces of the electrode to plate and that of the plate to plate<sup>8</sup>). When the reaction force acting on the spring is compressive the corresponding part of the interface is judged to be in-contact. If the interface is in-contact, the stiffness of the spring is set large enough to be considered as a rigid link.

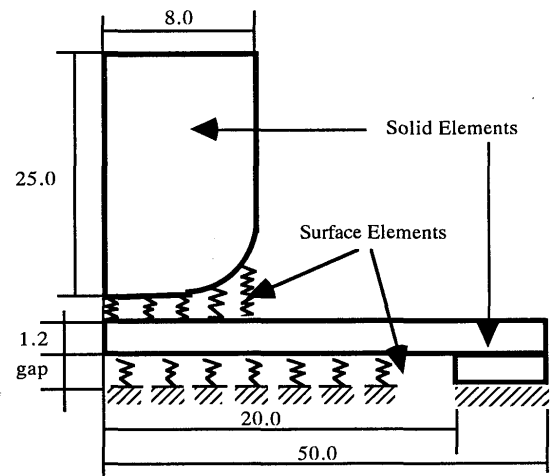
When the reaction force becomes tensile, the contact state is judged to be out-of-contact and the stiffness of the spring is set to be zero to cut the link. The transition from out-of-contact to in-contact is judged on the relative distance between nodes.

The forms of spot welding joints largely depend on the types of the structures. The full numerical analysis of the joints normally involves three dimensional problems. However, the problem is simplified as an axisymmetric problem in this paper. The model of the spot welding process with an initial gap is shown in Fig.1(a). Because of the symmetry, only one quarter of the model is analyzed as shown in Fig.1(b).

The dome-type electrode is used and its shape near the tip of the electrode is illustrated in the Fig.2. The tip



(a) spot welding model



(b) numerical analysis model

Fig 1 The numerical simulation model of spot welding process.

of dome-type electrode is spherical with its radius 40 mm within 3 mm from its center and it is tapered with radius 8 mm outside the spherical tip. The finite element mesh for the analysis model is shown in Fig.3 with 546 elements and 670 nodes including 46 surface elements. The initial gap is assumed to exist between plates.

The thickness of the plate to be welded is assumed to be 1.2 mm. The material used is mild steel. The melt temperature is 1480°C.

The material constants are dependent on temperature as shown in the following.

(1) The electrode (copper)

The yielding stress:

$$\begin{aligned} \sigma_s &= 20.0 & (T \leq 400^\circ\text{C}) \\ \sigma_s &= 41.6 - 0.054T & (400^\circ\text{C} < T \leq 750^\circ\text{C}) \\ \sigma_s &= 1.1 & (T > 750^\circ\text{C}) \end{aligned}$$

The Young's modulus:

$$\begin{aligned} E &= 13000.0 & (T \leq 0^\circ\text{C}) \\ E &= 13000.0 - 8.6T & (0^\circ\text{C} < T \leq 1500^\circ\text{C}) \\ E &= 100.0 & (T > 1500^\circ\text{C}) \end{aligned}$$

Thermal expansion ratio:

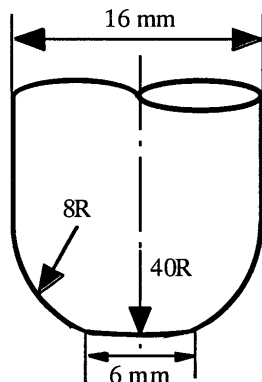
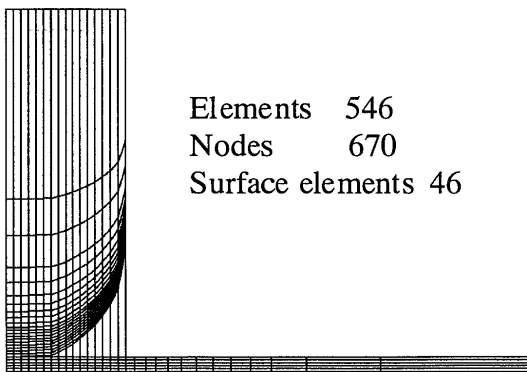


Fig.2 The dome-type electrode.



Elements 546  
Nodes 670  
Surface elements 46

Fig.3 The FEM mesh division for analysis model.

$$\alpha = 1.77 \times 10^{-5} \left( \frac{1}{^\circ\text{C}} \right)$$

The Poisson's ratio:

$$\gamma = 0.348$$

Thermal Conductivity:

$$\lambda = 0.314 \left( \frac{\text{J}}{\text{mm} \cdot \text{s} \cdot ^\circ\text{C}} \right)$$

Specific heat:

$$C = 0.389 \left( \frac{\text{J}}{\text{g} \cdot ^\circ\text{C}} \right)$$

Density:

$$\rho = 8.9 \times 10^{-3} \left( \frac{\text{g}}{\text{mm}^3} \right)$$

Heat conductivity:

$$\alpha_c = 0.314 \left( \frac{\text{J}}{\text{mm}^2 \cdot \text{s} \cdot ^\circ\text{C}} \right)$$

Resistibility :

$$\begin{aligned} \mu &= (0.0095 \times T + 1.79) \times 10^{-5} \\ & \quad (0^\circ\text{C} \leq T \leq 1083^\circ\text{C}) \\ \mu &= 12.08 \times 10^{-5} \quad (1083^\circ\text{C} < T) \end{aligned}$$

(2) The plate (mild steel)

The yielding stress:

$$\begin{aligned} \sigma_s &= 27.0 - 0.02T & (T \leq 500^\circ\text{C}) \\ \sigma_s &= 43.7 - 0.053T & (500^\circ\text{C} < T \leq 800^\circ\text{C}) \\ \sigma_s &= 1.0 & (T > 800^\circ\text{C}) \end{aligned}$$

The Young's modulus:

$$\begin{aligned} E &= 20000.0 & (T \leq 400^\circ\text{C}) \\ E &= 39900 - 49.75T & (400^\circ\text{C} < T \leq 800^\circ\text{C}) \\ E &= 100.0 & (T > 800^\circ\text{C}) \end{aligned}$$

Thermal expansion ratio:

$$\alpha = 1.28 \times 10^{-5} \left( \frac{1}{^\circ\text{C}} \right)$$

The Poisson's ratio:

$$\gamma = 0.30$$

Thermal Conductivity :

$$\begin{aligned} \lambda &= -3.487 \times 10^{-8} T^2 - 1.047 \times 10^{-5} T + 0.053 & (T \leq 400^\circ\text{C}) \\ \lambda &= -3.14 \times 10^{-8} T^2 - 4.187 \times 10^{-6} T + 0.00494 & (400^\circ\text{C} < T \leq 800^\circ\text{C}) \\ \lambda &= 0.00272 & (T > 800^\circ\text{C}) \end{aligned}$$

Specific heat :

$$\begin{aligned} C &= 1.285 \times 10^{-7} T^2 + 3.206 \times 10^{-4} T + 0.04 & (T \leq 400^\circ\text{C}) \\ C &= 7.746 \times 10^{-7} T + 0.475 & (400^\circ\text{C} < T \leq 600^\circ\text{C}) \\ C &= 3.070 \times 10^{-3} T - 1.089 & (600^\circ\text{C} < T \leq 750^\circ\text{C}) \\ C &= -5.443 \times 10^{-3} T + 5.296 & (750^\circ\text{C} < T \leq 850^\circ\text{C}) \\ C &= 0.6698 & (T > 850^\circ\text{C}) \end{aligned}$$

Heat conductivity:

$$\alpha_c = 0.314 \left( \frac{\text{J}}{\text{mm}^2 \cdot \text{s} \cdot ^\circ\text{C}} \right)$$

Specific heat :

$$C = 0.389 \left( \frac{\text{J}}{\text{g} \cdot ^\circ\text{C}} \right)$$

Density :

$$\rho = 7.8 \times 10^{-3} \left( \frac{g}{mm^3} \right)$$

Heat conductivity:

$$\alpha_c = 0.314 \left( \frac{J}{mm^2 \cdot S \cdot ^\circ C} \right)$$

Resistibility:

$$\begin{aligned} \mu &= (8.56 \times 10^{-5} T^2 + 0.049 T + 15.4) \times 10^{-5} \quad (T \leq 800^\circ C) \\ \mu &= (2.875 \times 10^{-2} T + 86.4) \times 10^{-5} \quad (800 < T \leq 1200^\circ C) \\ \mu &= 1.2 \times 10^{-3} \quad (T > 1200^\circ C) \end{aligned}$$

### 3. Result and Discussion

#### 3.1 Contact analysis

For spot welding with an initial gap, it is very important to understand the contact states at the interfaces of the electrode to plate (E/P contact) and the plate to plate (P/P contact) under squeezing force. The contact states of the interfaces would have large effect on electric current distributions and the size of nugget. The relationship between the squeezing force and the displacement at the center of the plate is shown in Fig.4. It can be seen that there exists a critical value of squeezing force for a given gap. If the squeezing force exceeds the critical value, contact will occur between plate and plate. The area with hatching in Fig.4 corresponds to the no-contact area. Of course, the contact area will expand as the squeezing force increases after the first contact occurs. Therefore, for an actual problem of spot welding with initial gap, the minimum squeezing force needed for contact can be obtained from Fig.4. This minimum squeezing force is dependent on the material properties and the dimensions of the model.

The contact states of P/E contact and P/P contact before and after squeezing are shown in Fig.5 for spot welding with 4.0mm initial gap and 200kgf squeezing force. The plates have a large deformation near the tip of electrodes.

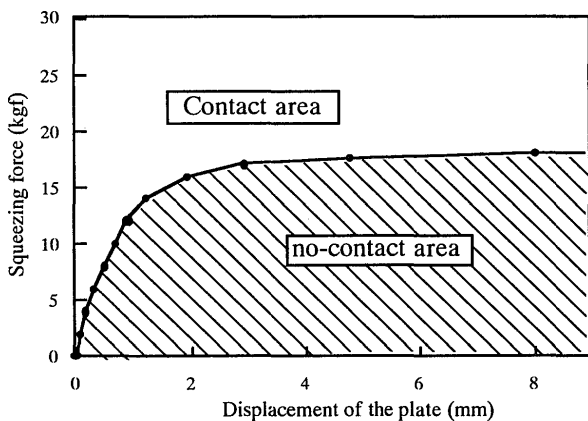


Fig.4 The relationship between squeezing force and displacement at the center of plate.

An enlargement of the contact states of the P/E and P/P is shown in Fig.6. It can be clearly seen that there exist a no-contact area for the E/P contact near the center of the electrode. The contact area is ring-like for the E/P contact and circular for the P/P contact. This feature of contact states is important to understand the process of the nugget initiation and growth. The parameters describing the ring-like area are drawn in Fig.6.

The development of contact area and nugget size with welding time for an initial gap 4.0mm is shown in Fig.7. The squeezing force is 200 kgf and current is 8000A. The line marked by bold triangles is the outside radius of the contact area between electrode and plate. The radius of contact increases with increasing welding cycle. The line marked by solid square represents the inside radius of the contact area between electrode and plate. The inside radius decreases with increasing welding cycles. It becomes zero when the welding cycles reach about 5. The changes of contact state between electrode and plate (E/P) can be described as follows. The ring-like contact state is made under the squeezing force. Then the ring-like contact area expands in both

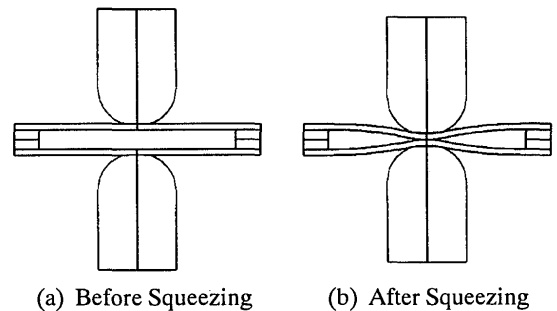


Fig.5 The contact state at interfaces with 4 mm initial gap before and after squeezing.

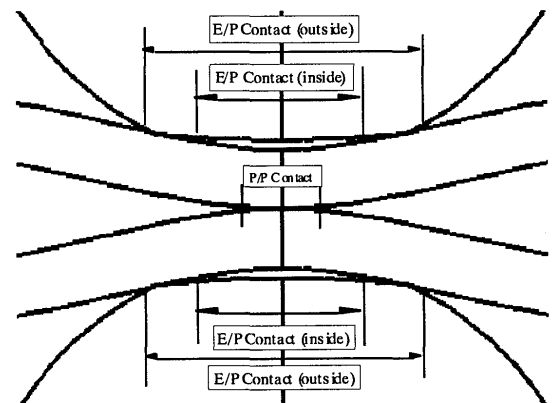


Fig.6 The contact state of electrode/Plate and plate/plate after squeezing.

inward and outward directions with an increase of welding time. The inside radius of the ring-like contact area will become zero after a certain welding time. The line marked by solid circles shows the contact radius between plate and plate (P/P). The contact area increase with increasing welding time. The lines marked by open squares and open circles denote the nugget radius and the nugget thickness, respectively. It is seen that the nugget diameter and the thickness will become constant after about 14 welding cycles even if the contact area is increasing.

The relationship between inside radius of contact area (E/P) and the initial gap is plotted in Fig.8. The squeezing force is 200 kgf. It can be seen that the inside contact radius increases with an increase of initial gap and becomes almost constant when the initial gap exceeds 2 mm. The squeezing force will affect the contact states in the squeezing process. The larger the

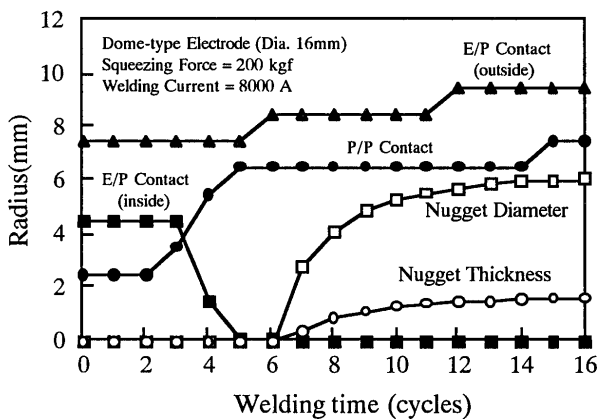


Fig. 7 The development of contact area and nugget sizes with welding time (initial gap 4.0 mm).

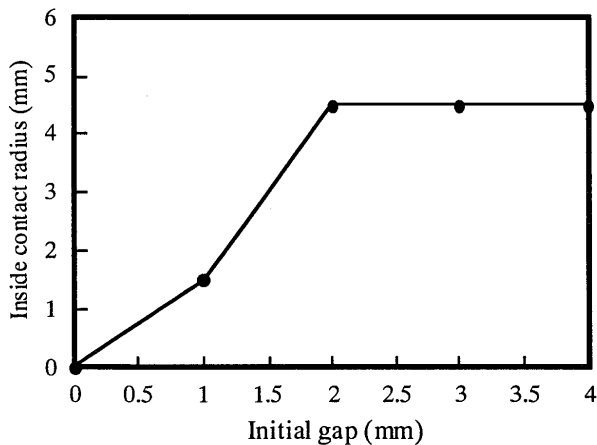


Fig. 8 The relationship between inside contact radius and initial gap.

squeezing force, the larger the inside radius is.

It is indicated in Fig.9 that the inside contact radius will decrease with increase of welding time because the material becomes softer as the temperature increases. The squeezing force is 200 kgf in the calculation. The inside contact radius becomes zero after about 4 or 5 welding cycles in this case.

### 3.2 Nugget formation

The temperature distribution during spot welding with 4.0 mm initial gap after 12 welding cycles is shown in Fig.10. The squeezing force is 200 kgf. The nugget dimensions and Heat Affected Zone can be seen from this figure.

The development of the nugget diameter and the nugget thickness with welding time (cycles) for different initial gap is illustrated in Fig.11. The squeezing force is 200 kgf. It can be seen that the nugget diameters and nugget thicknesses are almost the same after about 14 welding cycles with or without the initial gap. The initial formation of the nugget is delayed by the initial gap and the formation time is almost the same when the initial gap exceeds 1.0 mm.

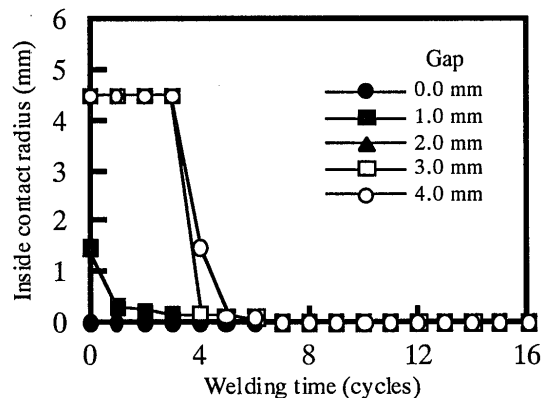


Fig. 9 The relationship between inside contact radius and welding time.

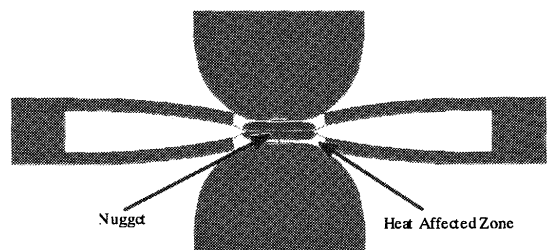


Fig. 10 The simulated nugget size with 4.0 mm initial gap after 12 welding cycles.

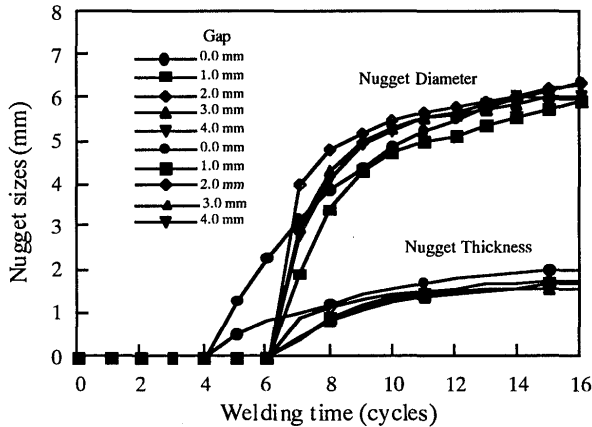


Fig.11 The development of nugget diameter and thickness with welding time for different initial gap.

The development of nugget diameter and nugget thickness with welding time is shown in Figs.12 and 13 for different welding currents. The squeezing force and the initial gap are assumed as 200kgf and 2.0 mm, respectively. The abscissa and the ordinate show the welding time (cycles) and nugget dimensions. It can be seen that the nugget diameter and nugget thickness are dependent on the welding current. The initial formation of nugget is significantly delayed by a decrease of welding current. The nugget would not be formed in a case where the welding current was less than 6000A. The increasing tendency of nugget diameter is larger than that of nugget thickness after 10 welding cycles.

The development of nugget diameter and nugget thickness with different squeezing force is shown in Figs.14 and 15. The welding current and the initial gap are assumed as 8000A and 2.0 mm, respectively. It can be seen from Figs.14 and 15 that the nugget diameter and the nugget thickness are dependent on the squeezing force. The formation of nugget is delayed somewhat as the increase of squeezing force. The larger the squeezing force, the later the nugget formation is.

The effects of the welding current on the nugget diameter and the nugget thickness are shown in Figs.16 and 17 after 8, 12, and 16 welding cycles, respectively. The nugget diameter and the nugget thickness increase with increasing welding current. The differences of nugget dimensions between 8 and 16 cycles become smaller as the welding current increases. The nugget thickness at 8 and 16 cycles becomes almost constant when the welding current exceeds 10000A. That means that for a given welding current there exists a welding time (cycle) to get the maximum nugget. The longer the heating time, the larger the crystal size will become for

steels sensitive to heating. This conclusion is very important for the spot welding of steels sensitive to heating time in order to get weld joints with good quality.

The nugget diameter and the nugget thickness with different squeezing forces are shown in Figs.18 and 19 after 8, 12, and 16 welding cycles, respectively. The nugget diameter and the nugget thickness decrease as the squeezing force increases. The change of nugget dimensions with squeezing force becomes smaller with an

increase in welding time. This means that the time for the nugget to grow to a certain size becomes larger with an increase of squeezing force in case of the spot welding with initial gap. Therefore, it may be very important to control the squeezing force for the spot welding of steels sensitive to heating time. If the steel is sensitive to heating time, it is better to reduce the welding time for spot welding.

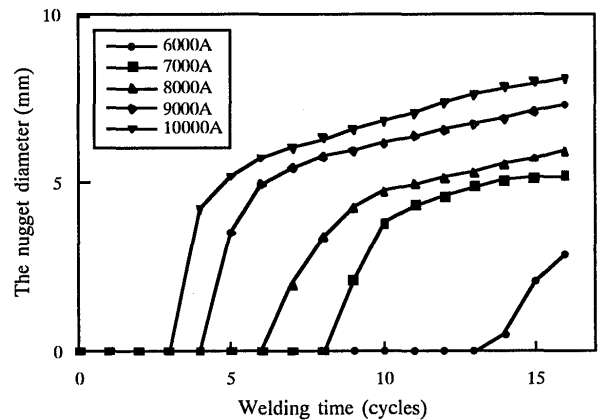


Fig.12 Development of nugget diameter with welding time for different currents (initial gap 2.0mm).

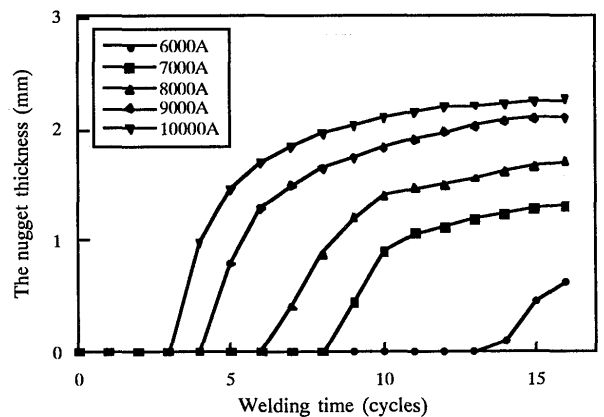


Fig.13 Development of nugget thickness with welding time for different currents (initial gap 2.0 mm).

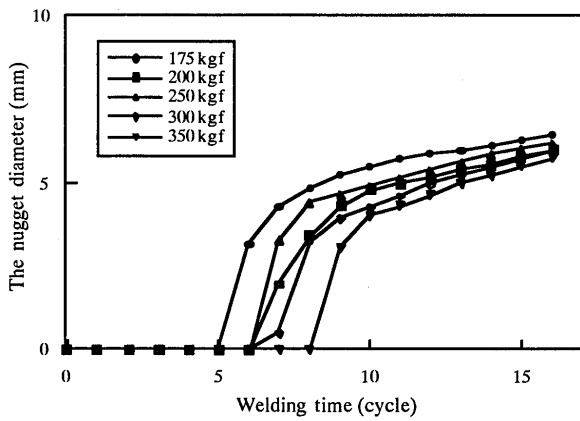


Fig. 14 Development of nugget diameter with welding time for different loads (initial gap 2.0mm).

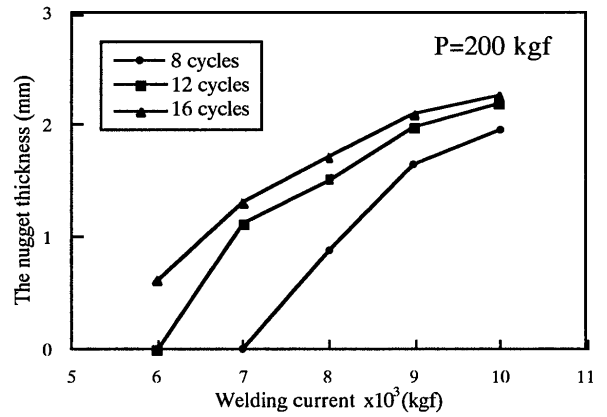


Fig. 17 Effect of the welding current on the nugget thickness.

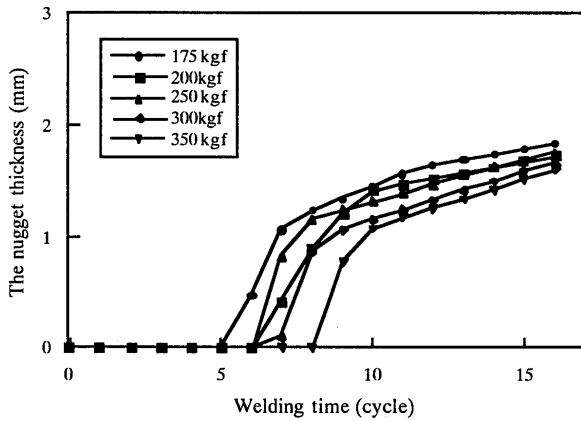


Fig. 15 Development of nugget thickness with welding time for different loads (initial gap 2.0 mm).

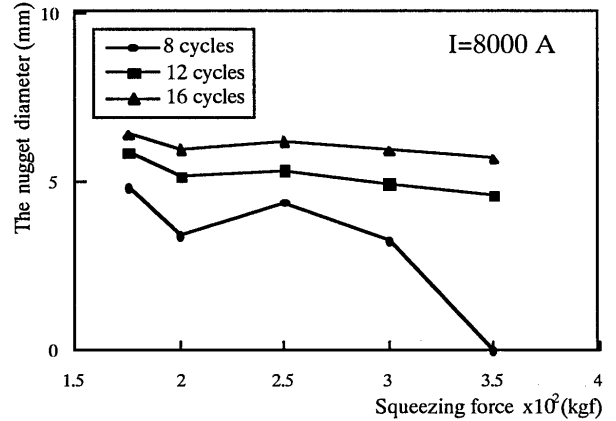


Fig. 18 Effect of the squeezing force on the nugget diameter.

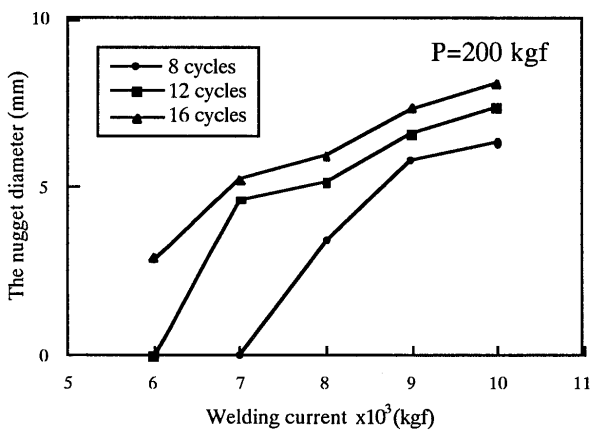


Fig. 16 Effect of the welding current on the nugget diameter.

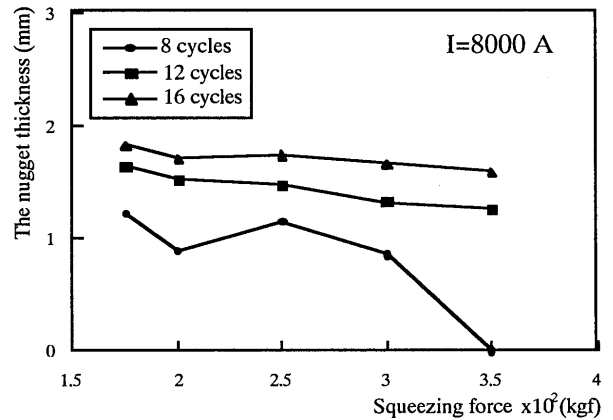


Fig. 19 Effect of the squeezing force on the nugget thickness.



## FEM Simulation of Spot Welding Process

### 4. Conclusion

Based on a finite element program developed for analyzing the spot welding process, the contact states and nugget formation of mild steel in spot welding with initial gap were analyzed. The conclusions are the following.

For the spot welding with initial gap, the ring-like contact state between electrode and plate can be formed under the squeezing force, and the contact area develops in inward and outward directions as the welding time increases.

The formation of the nugget is delayed by the initial gap. The formation time is almost the same when the initial gap exceeds 1.0 mm. The formation of nugget is also delayed as the welding current decreases. The nugget diameter and the nugget thickness increase with increase of welding current. The initial formation of the nugget is delayed somewhat as the increase of squeezing force. The nugget diameter and the nugget thickness decrease with an increase of squeezing force. The change of nugget dimensions with squeezing force becomes smaller with an increase of welding time. It means that the time for the nugget to grow to a certain size becomes larger with an increase of the squeezing force in case of spot welding with initial gap.

### References

- 1) W.Rice, and E.J.Funk, "Analytical investigation of the temperature distribution during resistance welding", *Welding Journal*, Vol.46, No.4, (1967), 175s-182s.
- 2) K.C.Wu, "Resistance spot welding of high contact-resistance surfaces for weldbonding", *Welding Research Supplement*, Dec.1975, 436s-443s.
- 3) D.W.Dickinson, J.E.Franklin, and A.Stanya, "Characterization of spot welding behaviour by dynamic electrical parameter monitoring", *Welding Journal*, Vol.59, No.6, (1980), 170s-176s.
- 4) J.M.Sawhill, and J.C.Baker, "Spot weldability of high-strength sheet steels", *Welding Journal*, Vol.59, No.1, (1980), 19s-30s.
- 5) J. A. Greenwood, "Temperatures in spot welding", *British Welding Journal*, (1961), 316-322.
- 6) H.A.Nied, "The Finite Element Modeling of the Resistance Spot Welding Process", *Welding Research Supplement*, April 1984, 123-132.
- 7) C.L. Tsai, O.A.Jammal, J.C.Papritan, and D.W. Dickinson, "Modeling of resistance spot welding nugget growth", *Welding Research Supplement*, Feb. 1991, 47s-54s.
- 8) H. Murakawa, H. Kimura, and Y. Ueda, "Weldability Analysis of Spot Welding on Aluminum Using FEM", *Trans. JWRI*, Vol.24, No.1, (1995), 101-111.
- 9) C.L. Tsai, W.L. Dai, D.W. Dickinson and J.C.Papritan, "Analysis and Development of a Real-Time Control Methodology in Resistance Spot Welding", *Welding Research Supplement* Dec. 1991, 339-351.
- 10) K.Nishiguchi, K.Matruyama and T.Myouga, "Fundamental Study on Spot Welding of Pressformed Members - influences of initial gap and yielding strength of materials -", *Japan Welding Society, Technical Commission on Resistance Welding, Report RW-199-81*, 1981, (in Japanese).
- 11) H.Murakawa and Y.Ueda, "Mechanical Study on the Effect of the Initial Gap upon the Weldability of Spot Weld Joint", *Trans. JWRI*, Vol.18, No.1, (1989),51-58